

Physics of Solutions and Networks of Semiflexible Macromolecules and the Control of Cell Function *

ERWIN FREY, KLAUS KROY AND JAN WILHELM

Contents

1	Introduction	1
2	Single Chain Properties	3
2.1	Force-Extension Relation	3
2.2	Radial Distribution Function	4
2.3	Dynamic Light Scattering	5
3	Collective Properties	6
3.1	Plateau Modulus for Entangled Solutions	6
3.2	Viscoelasticity and High Frequency Behavior	8
3.3	Effect of crosslinking	9
4	Summary and Future Perspectives	10

1 Introduction

Most of the concepts used to understand the viscoelastic properties of chemical and physical gels of *flexible* polymers require the persistence length ℓ_p [1] to be significantly smaller than other characteristic scales such as the filament length L , the distance between crosslinks or the width of reptation tubes. This condition no longer holds for networks of *semiflexible* polymers. One prominent family of such polymers are cytoskeletal biopolymers like F-actin, intermediate filaments and microtubules. An impression of the typical conformations of the filaments and the relative magnitude of the characteristic length scales can be gained upon inspection of the following electron micrograph of a semidilute actin solution. The most striking features of these networks are the enormous length and relatively elongated structures of the constituent biopolymers. Actin filaments have a diameter of 7 nm [2] and can reach lengths up to 30-100 μm *in vitro* [3], and several microns *in vivo*. The persistence length is approximately 17 μm [4, 5, 6], quite large compared to typical distances between neighboring filaments which is in the range of a few tenth of a micron. This combination of length scales allows biopolymers to form networks at very low volume fraction, so that solutions of less than 0.1% volume fraction of polymer are still strongly entangled. Thus only a small amount of material needs to be produced by the cell in order to generate a sufficiently strong network. This fact

*Expanded version of an invited talk given at the 14th Polymer Networks Group International Conference in Trondheim (Norway), June 28 - July 3. Published in *The Wiley Polymer Networks Group Review Series, Volume 2*

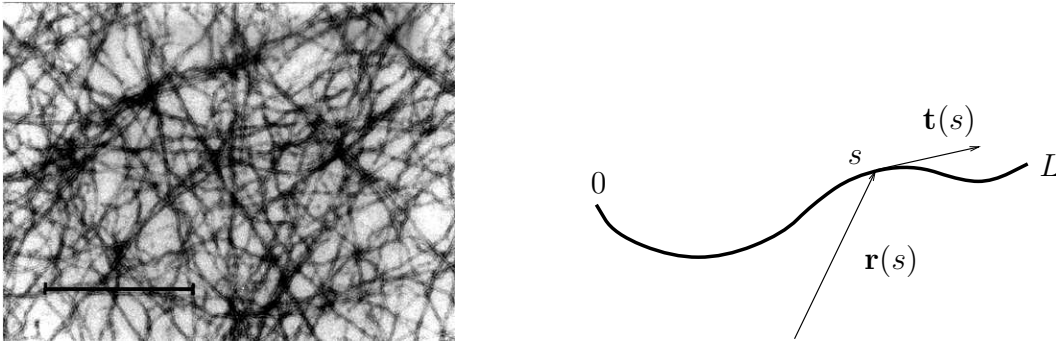


Figure 1: *Left:* Electron micrograph of a 0.4 mg/ml actin solution. The bar indicates 1 μm . *Right:* Sketch of the wormlike chain as a space curve $\mathbf{r}(s)$.

is not only of considerable biological relevance but also facilitates interpretation of dynamic light scattering experiments and their relation to theory [7, 8].

There are several motivations [9, 10, 11, 12] for studying the viscoelasticity of cytoskeletal networks [13, 14, 15, 16, 17, 18, 19, 20, 21, 22]:

(I) From a polymer physics perspective they are interesting because their behavior is expected to be determined by principles and mechanisms different from those established for flexible networks. In fact much of the physics behind the viscoelasticity of semiflexible polymer networks is only being explored recently [23, 24, 25, 26, 27, 28, 29, 30].

(II) From an experimental point of view, semiflexible polymer networks are interesting because several semiflexible polymers have persistence lengths on the order of several μm or even mm. Thus techniques such as optical microscopy of single fluorescence labeled filaments or attached colloidal probes can be used to study the behavior of the network at the *single polymer level* [18, 19, 22, 31]. For flexible polymers this has been possible only in simulations (see, e.g., [32]).

(III) Finally, the viscoelastic properties and regulation of semiflexible polymer networks both inside cells and in the extracellular matrix are of significant importance for the mechanical stability and properties of biological tissue, for cell locomotion, adhesion and force generation [9, 10, 11].

The Cytoskeleton: Structure and Biological Role

Living cells need both the ability to maintain their shape when exposed to shear stresses exerted by their active contractile machinery or by fluid flow in blood vessels and the ability to reorganize their shape and internal architecture as is the case in cell migration and mitosis. The structure responsible for the mechanical and dynamic properties of the cell is the *cytoskeleton*, a rigid yet flexible and *dynamic network of proteins* of varying length and stiffness. Most eukaryotic cells contain three types of protein filaments comprised of *actin*, *tubulin* and *intermediate filament proteins* such as vimentin. These, as well as the plasma-membrane associated filaments make up the cytoskeleton [33]. There is also a range of *accessory proteins* for each of the cytoskeletal filaments which allow for *control* of nearly all mechanically relevant properties of the protein filaments [34, 35]. Let us just mention one exam-

ple, gelsolin, which is frequently used in rheological experiments. It caps the end of a growing actin filament and can thus be used to regulate the average filament length in actin solutions. There are many other proteins with different tasks ranging from initiating and terminating polymerization over introducing crosslinks and forming lateral arrays of filaments to even changing the stiffness of the filaments.

An example of the biological role of the cytoskeleton is the migration of an amoeba. Its motion is initiated by adhesion driven spreading of the cell membrane on the substrate followed by gelation of actin in the advancing lobe (pseudopodium). The cycle is completed by retraction of the rear end and a gel-sol transition or fiber formation in the advancing front [11]. This process is of course quite complex and there is a subtle interplay between regulatory mechanisms and the material properties of the cytoskeleton. But, understanding the basic physical principles determining the viscoelasticity of actin networks is certainly a prerequisite in understanding such a biological process. In the following we will address the following questions: (i) Can we even understand the physics of a one-component system such as a purified F-actin solution (depicted in Fig. 1)? (ii) Can we identify the basic physical principles underlying the observed viscoelastic behavior? (iii) How is it different from the physics of long flexible coils?

2 Single Chain Properties

The model usually adopted for a theoretical description of semiflexible chains is the *wormlike chain model* [1, 36]. Here one describes the filament as a smooth inextensible line $\mathbf{r}(s)$ of length L parameterized in terms of the arc length s . The statistical properties are determined by an effective free energy (the ‘‘Hamiltonian’’)

$$\mathcal{H}(\{\mathbf{r}(s)\}) = \frac{\kappa}{2} \int_0^L ds \left(\frac{\partial^2 \mathbf{r}(s)}{\partial s^2} \right)^2, \quad (1)$$

which measures the total elastic energy of a particular conformation by the integral over the square of the local curvature weighted by the *bending modulus* κ . The inextensibility of the chain is expressed by the local constraint, $|\mathbf{t}(s)| = 1$, on the tangent vector $\mathbf{t}(s) = \partial \mathbf{r} / \partial s$. We will see that this constraint is essential for a correct description of the static as well as the dynamic properties of semiflexible polymers. Due to the mathematical complications resulting from the inextensibility only few of the statistical properties of the wormlike chain can be extracted analytically, the best known being the exponential decay of the tangent-tangent correlation function $\langle \mathbf{t}(s) \mathbf{t}(s') \rangle = \exp(-|s - s'| / \ell_p)$ with the persistence length $\ell_p = \kappa / k_B T$, the mean-square end-to-end distance [1] $\mathcal{R}^2 := \langle [\mathbf{r}(L) - \mathbf{r}(0)]^2 \rangle = L^2 f_D(L / \ell_p)$, and the radius of gyration [37] $\mathcal{R}_g^2 = \ell_p^2 (f_D(L / \ell_p) - 1 + L / 3\ell_p)$, where $f_D(x) := 2(e^{-x} - 1 + x) / x^2$ is the Debye function.

2.1 Force-Extension Relation

One of the most obvious differences between flexible and semiflexible polymers is their response to external forces (see Fig. 2 (left)). In the flexible case the response

is isotropic and proportional to $1/k_B T$, i.e., the Hookian force coefficient is proportional to the temperature. When the persistence length is of the same order of magnitude as the contour length, the response becomes increasingly *anisotropic*.

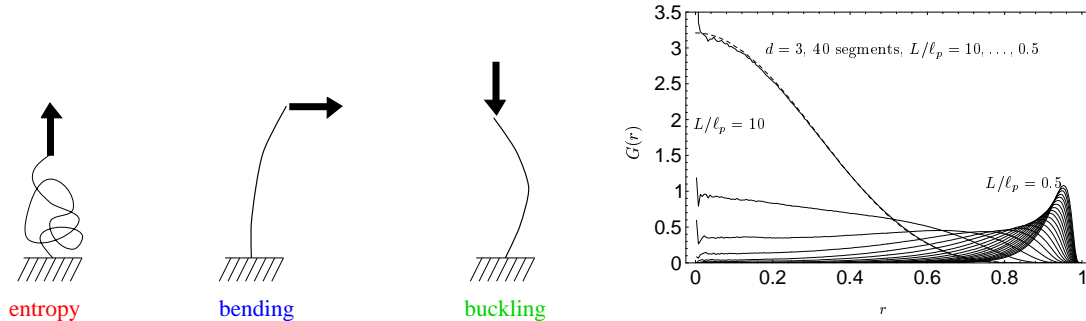


Figure 2: *Left*: A flexible chain’s linear response is purely entropic and isotropic. The elastic response of a stiff rod is extremely anisotropic. Transverse forces (bending) lead to a purely mechanical response, whereas the longitudinal response (buckling) is characterized by a spring constant inversely proportional to the temperature. *Right*: Numerical results for the end-to-end distribution function of a (discretized) wormlike chain in $d = 3$ dimensional space (numerical data from Ref. [38]). With increasing stiffness there is a pronounced crossover from a Gaussian shape to a form with the weight shifting towards full stretching. The dashed line indicates the Daniels approximation [39].

Then the linear response of the chain depends on the orientation of the force with respect to the tangent vector at the clamped end. Transverse forces give rise to ordinary mechanical bending of the filaments and the *transverse spring coefficient* is proportional to κ . The linear response for longitudinal forces is due to the presence of thermal undulations, which tilt parts of the polymer contour with respect to the force direction. The effective *longitudinal spring coefficient* turns out to be proportional to κ^2/T indicating the breakdown of linear response at low temperatures ($T \rightarrow 0$) or very stiff filaments ($\ell_p \rightarrow \infty$). This is a consequence of the Euler buckling instability. Note also that for the special boundary conditions of a grafted chain (as depicted in Fig. 2 (left)) the linear response of the chain can even be worked out exactly for arbitrary stiffness [27]; these calculations use the fact that the conformational statistics of the wormlike chain is equivalent to the diffusion on the unit sphere [36].

2.2 Radial Distribution Function

An important quantity describing the statistical properties of the chain is the *probability distribution of the end-to-end vector* $G(\mathbf{r}; L) = \langle \delta(\mathbf{r} - \mathbf{R}) \rangle$. For a *freely jointed phantom chain* this function is known exactly [40]. As for any model with short-ranged interactions it converges quickly to a Gaussian distribution $G_0(\mathbf{r}; L) \sim \exp(-3r^2/4\ell_p L)$ for an increasing number of segments. For chains that are at least some $10\ell_p$ long the Gaussian can serve as an excellent approximation to $G(\mathbf{r}; L)$ for many purposes. For the freely jointed chain the persistence length ℓ_p is independent of temperature because its microscopic origin lies in steric constraints rather than in the bending stiffness of the backbone.

For a Gaussian chain, the separation by a given distance r of any two segments with preferred mean-square distance $2\ell_p s$ is punished by the free energy cost $F(\mathbf{r}) = -k_B T \ln G_0(\mathbf{r}; s) = \text{const.} + 3k_B T \mathbf{r}^2 / 4\ell_p s$ quadratic in the end-to-end distance. Due to the Euler instability this is very different for semiflexible chains. The characteristic feature of the physics of beam buckling is that the energy E_{cl} of a straight rod is an almost *linear* function of its end-to-end distance R , $E_{\text{cl}} \approx f_c \cdot (L - R)$. Here $f_c = \kappa \pi^2 / L^2$ is the critical force for the onset of the Euler instability. Neglecting fluctuations around the classical contour this would lead to an end-to-end distribution function with maximum weight at $R = L$, $G(\mathbf{r}; L) \propto \exp[-f_c \cdot (L - r) / k_B T]$. Note that with such an approach we completely ignore entropic effects which are the only contributions in case of the freely jointed chain, discussed above. In order to correct for this omission we have to multiply the above Boltzmann weight by the relative number of allowed conformations. This becomes most obvious for a completely stretched chain, where up to global rotations only one possible configuration exists and consequently the end-to-end distribution function has to vanish. These qualitative arguments lead to the shape of the distribution function shown in Fig. 2 (right). The actual form of the end-to-end distribution function can be obtained within a quantitative analysis [38] of the wormlike chain.

2.3 Dynamic Light Scattering

A useful experimental technique for investigating the short time dynamics of semiflexible polymers is dynamic light scattering (DLS). In DLS experiments one directly observes the dynamic structure factor $g(\mathbf{q}, t)$. We focus on the ideal case of a dilute or semidilute solution of semiflexible polymers, where the scattering wavelength is much smaller than the mesh size. We also assume a separation of length scales, $a \ll \lambda \leq \ell_p, L$, i.e., the scattering wavelength λ is large compared to the monomer size a but small compared to the characteristic mesoscopic scale defined by L and ℓ_p . As a consequence the contributions to the time decay of $g(\mathbf{q}, t)$ from center of mass and rotational degrees of freedom of the chain are strongly suppressed as compared to contributions from bending undulations. Moreover, for this case [41, 42, 43, 7, 30] the structure factor can be written as $\exp(-q^2 r_{\perp}^2(t) / 4)$ with the local mean square displacement $r_{\perp}^2(t) \sim t^{3/4}$:

$$g(\mathbf{q}, t) \propto \exp[-(\gamma_q t)^{3/4}], \quad (2)$$

where $\gamma_q \sim q^{8/3} / \zeta_{\perp} \ell_p^{1/3}$ [7, 8]. Such a stretched exponential behavior has been confirmed experimentally with very high accuracy for F-actin solutions [44]. However, a more careful analysis reveals that it cannot hold for very short times. For times shorter than $\zeta_{\perp} / \kappa q^4$ the bending forces can be considered weak and the contour obeys the fast wiggling motion imposed by hydrodynamic fluctuations. As a consequence the initial decay is of the form $g(\mathbf{q}, t) \propto \exp(-\gamma_q^{(0)} t)$ with [7]

$$\gamma_q^{(0)} = \frac{2k_B T}{3\pi \zeta_{\perp}} q^3 = \frac{k_B T}{6\pi^2 \eta} q^3 \ln(e^{5/6} / ka). \quad (3)$$

For polymers, which are not quite as stiff as actin, e.g. for so called intermediate filaments, this initial decay regime is readily observed in light scattering experiments.

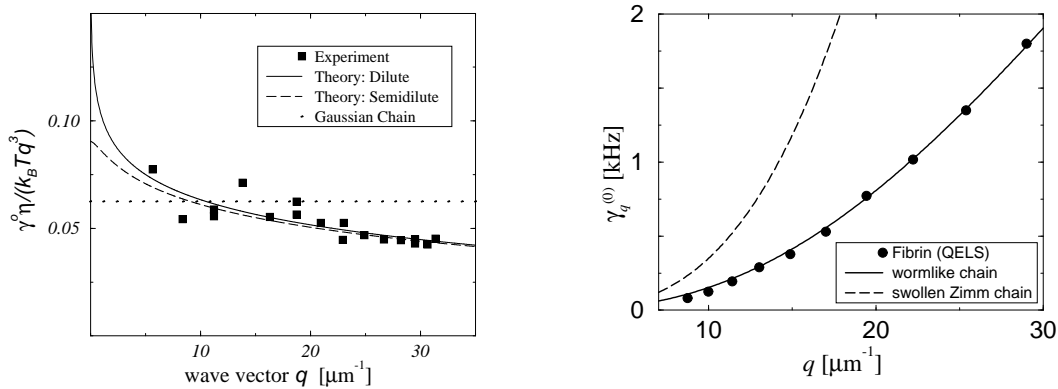


Figure 3: *Left*: The q -dependence of the initial decay rate compared to DLS data on actin [45]. *Right*: Comparison of the classical result for a swollen Zimm chain [46] with Eq. (3) and quasi-elastic light scattering experiments with the semiflexible biopolymer fibrin [47]. The data were most kindly provided by G. Arcovito (see also this volume).

A very convincing confirmation of these theoretical results has recently been found in fibrin systems [47] (see Fig. 3). Analyzing the data by Eq. 3 allows one to estimate the friction coefficient ζ_{\perp} entering the Langevin equation or, equivalently, the thickness a of these filaments.

3 Collective Properties

In conventional polymer systems made up of long flexible chain molecules the viscoelastic response is *entropic* in origin over a wide range of frequencies [46]. For semiflexible polymers a complete understanding of the viscoelastic response is complicated by several factors. First of all, there are several ways by which forces can be transmitted in a network. This can either happen by steric (or solvent-mediated) interactions between the filaments or by viscous couplings between the filaments and the solvent undergoing shear flow. It is a priori not at all obvious which if any of these coupling will dominate. In the case of flexible polymers it is generally believed that macroscopic stresses are transmitted in such a way that these transformations stay affine locally, i.e. that the end-to-end distance of a single filament follows the macroscopic shear deformation [46]. Second, single filaments are *anisotropic elastic elements* showing quite different response for forces perpendicular or parallel to its mean contour. Therefore one has to ask what kind of deformation of the actin filament is the dominant one and whether due to the anisotropy of the building blocks of the network macroscopically affine deformations stay affine locally. In the following we will address some of the issues raised.

3.1 Plateau Modulus for Entangled Solutions

If solutions of semiflexible polymers are sufficiently dense and are probed on sufficiently short time scales (typically in the range of 10^{-2} Hz to 1 Hz) they will exhibit a “*rubber plateau*”. Its existence is in general traced back to a *time scale separation*

between the internal dynamics and the center of mass motion of the polymers. An externally imposed shear stress will then be transmitted to the individual strands, whose response will determine the magnitude of the modulus. This many chain problem is usually reduced to a single chain model by making certain assumptions on the effect of the mutual steric constraints on the conformation of a single filament.

In what might be called the *affine model* the “phantom model” [48] is adopted to semiflexible polymer systems [25]. It is assumed that upon deforming the network macroscopically the path of a semiflexible polymer between two entanglement points is straightened out or shortened in an affine way with the sample. The macroscopic modulus is then calculated from the free energy cost associated with the resulting change in the end-to-end distance. Since in a solution forces between neighboring polymers can only be transmitted transverse to the polymer axis and there is no restoring force for sliding of one filament past another, it is however hard to imagine that entanglements are able to support longitudinal stresses in filaments. The modulus predicted in the affine model should scale as $G^0 \propto c^{11/5}$ and leads to absolute values of the order of 10 Pa; such high values are at odds with the low values observed in recent experiments on F-actin solutions [49]. It was therefore argued [12] that such models are more appropriate for crosslinked networks, where they would predict a plateau value $G^0 \simeq k_B T \ell_p^2 / \xi_m^5$. But, even in such chemical networks with crosslinks present it is a priori not obvious that local deformations on the scale of a single filament are actually affine and that longitudinal stresses in the filaments are the dominant contribution to the plateau modulus (see also section 3.3).

Recent theoretical and experimental studies [26, 49] based on Refs. [50, 51, 52] suggest a different view. Here one considers the free energy cost of suppressed transverse fluctuations of the polymers that comes about by an *affine deformation of the tube* diameter. According to Odijk [51] the mean distance between collisions of a tagged polymer with its surrounding tube with diameter d is given by the deflection length $L_e \simeq \ell_p^{1/3} d^{2/3}$. Since each of these collisions reduces the conformation space there is a free energy of the order of $k_B T$. The total free energy of $\nu = c/L$ polymers per unit volume becomes $F \simeq \nu k_B T L / L_e$. To be able to compare these results to experiments one needs to know how the tube diameter d depends on the concentration of the solution or equivalently on the mesh size $\xi_m := \sqrt{3/\nu L}$. In other words we have to determine the average thickness d of a bend cylindrical tube in a random array of polymers as depicted in Fig. 4 (left).

The contour and thickness of the tube will be determined by a competition between bending energy favoring a thin straight tube and entropy favoring a curved thick tube. This competing effects define a characteristic length scale which turns out to be L_e . For length scales below L_e the tube will be almost straight and we can estimate its thickness as follows. Upon restricting the orientations of the polymers to being parallel to the coordinate axes the density of intersection points (black dots in Fig. 4) (left) will be $1/\xi^2$. Hence for a tube of length L_e the line density of these intersection points projected to a line perpendicular to the tube increases as L_e/ξ_m^2 which implies that the tube diameter decreases with increasing tube length as $d \simeq \xi_m^2 / L_e$. Hence one finds $L_e = (\xi_m^2 \ell_p^{1/2})^{2/5}$ leading to the following form of the

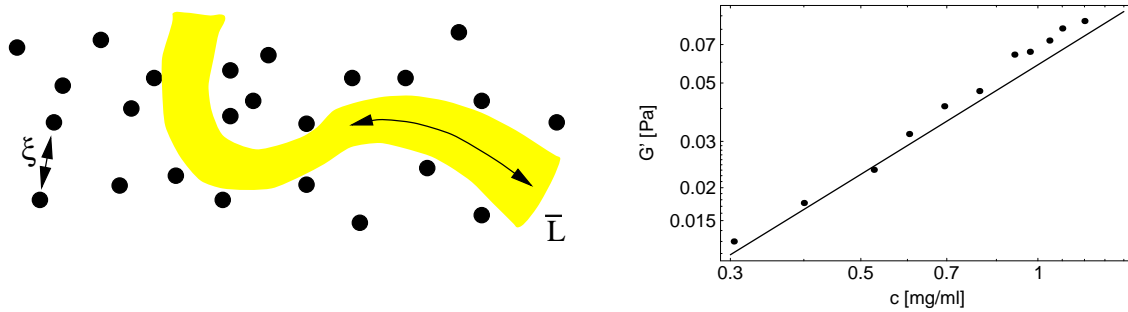


Figure 4: *Left:* A semiflexible polymer can trade bending energy for a wider tube. The configuration of the constraining polymers (dots) is the same as in the upper figure. *Right:* Comparison of the predicted shear modulus [53] to experiment [21]. The total length L and persistence length ℓ_p were set to $\ell_p = 17 \mu\text{m}$ and $L = 16 \mu\text{m}$, respectively [21].

free energy and hence the plateau modulus

$$G^0 \simeq F \simeq k_B T \ell_p^{-1/5} c^{7/5}. \quad (4)$$

The above scaling law is included as a limiting case in a more detailed analysis concerned with the calculation of the absolute value of the plateau modulus [53]. The same scaling result has been obtained previously [26] using a different scaling argument.

Recent experiments seem to favor the above tube picture, where the plateau modulus is thought to arise from free energy costs associated with deformed tubes due to macroscopic stresses. Fig. 4 (right) shows the results of a recent measurement of the concentration dependence of the plateau modulus in F-actin solutions [49] which agrees well with the scaling prediction $G^0 \propto c^{7/5}$.

3.2 Viscoelasticity and High Frequency Behavior

At frequencies above the “rubber plateau” (i.e. above 1 Hz for a typical F-actin solution) a power-law increase of the storage and loss modulus with frequency, $G'(\omega) \propto G''(\omega) \propto \omega^{3/4}$, has been observed [54, 55, 56]. It is tempting to speculate that it is somehow tightly connected with the anomalous subdiffusive behavior of the segment dynamics of a single filament. But in view of the actual micro-rheological experiments, where one observes the mean-square displacement of a bead of diameter larger than the mesh size and hence couples to a large number of filaments, it is not obvious how this comes about. A thorough understanding would need to explore the nature of the crossover from local dynamics dominated by filament undulations to the collective dynamics of the network and the solvent.

At present there are two different theoretical approaches based on different assumptions on the nature of the dominant excitations of the individual filaments generated by the beads embedded in the network. In one class of theoretical models one takes over the above mentioned “phantom model” to the high frequency behavior [57, 58]. It is assumed that under an applied shear deformation the filaments

undergo affine deformations on a length scale of order L_e implying longitudinal stresses on single filaments. In the high frequency regime this leads to [57, 58]

$$G^*(\omega) = \frac{1}{15} \nu (k_B T)^{1/4} \ell_p^{5/4} (i\omega \zeta_\perp)^{3/4}, \quad (5)$$

independent of the entanglement length L_e .

A complementary theoretical approach [59] starts from an effective medium description for the polymer solution at large scales which crosses over to the single polymer picture at about the tube diameter. The low frequency response is due to peristaltic modes of the effective medium. At high frequencies, the penetration depth for these modes falls below the tube diameter and the excitations are bound to the polymer backbones. Assuming that the forces between polymers are transmitted by binary collisions, the transverse modes that make up the plateau modulus according to the tube model, are also responsible for the high frequency response. This again leads to an $\omega^{3/4}$ -asymptotics of $G^*(\omega)$ at high frequencies. However, the model describes the crossover to and the moduli within the plateau region and allows scaling predictions for the relationship between plateau modulus and entanglement frequency. The information contained in the viscoelastic moduli is conveniently expressed in terms of the density of relaxation modes. Preliminary investigations show that already the simplest scaling assumption for this density (which certainly greatly over-simplifies the complicated crossover from single polymer dynamics to the effective medium modes) leads to excellent agreement with experimental data. Using the fluctuation-dissipation theorem, the long time behavior of the dynamic structure factor in semidilute solutions can also be derived.

Which one of these theoretical models is capturing the correct physics is not clear at present. It may well be that the actual physical mechanism is different from both. There is certainly a tremendous need for more detailed experimental studies which not only measure the power-law dependence of the modulus but also determine the concentration dependence of the entanglement frequency.

3.3 Effect of crosslinking

For a crosslinked network of semiflexible polymers bending *and* compressing forces can be transmitted to the filaments. Both for networks where the mesh size is very small compared to the persistence length so that the longitudinal elastic response of the polymers is dominated by their Young's modulus and for networks with larger mesh size where thermal undulations are crucial in understanding the elastic response of single filaments [25, 27], compression is a much stiffer mode of deformation than bending. Unless highly ordered network geometries are assumed, it is not clear which of the two modes will dominate the elastic response. Different assumptions on the real or effective network geometry can either favor the bending modes as in [28] or the compressional modes as in [25] leading to substantially different predictions for the modulus.

We used a two-dimensional toy model to investigate which type of deformation mode is dominant in a disordered crosslinked network. Sticks of length L were placed randomly on the plane and crosslinked at every intersection with another

stick. Crosslinks were inextensible. Sticks were assigned a Young's modulus E and a diameter r resulting in force constants $k_{\text{comp}} = \pi r^2 E$ for compression and $k_{\text{bend}} = 3\pi r^4 E/3L^2 = 3\kappa/L^2$ for bending the rod with one end clamped. Units were chosen such that $L = 1$ and $\kappa = 1$. The model was subjected to periodic boundary conditions, strained and the linear elastic response calculated by the method of finite elements. While this is a purely mechanical model it captures the essential features of two very different force constants and disorder. Entropic contributions from fluctuations of the crosslink positions are not expected to be significant for dense networks.

Which of the two modes dominates the elastic behavior was determined by keeping k_{bend} fixed and varying k_{comp} . We observe that for slender rods or low densities a

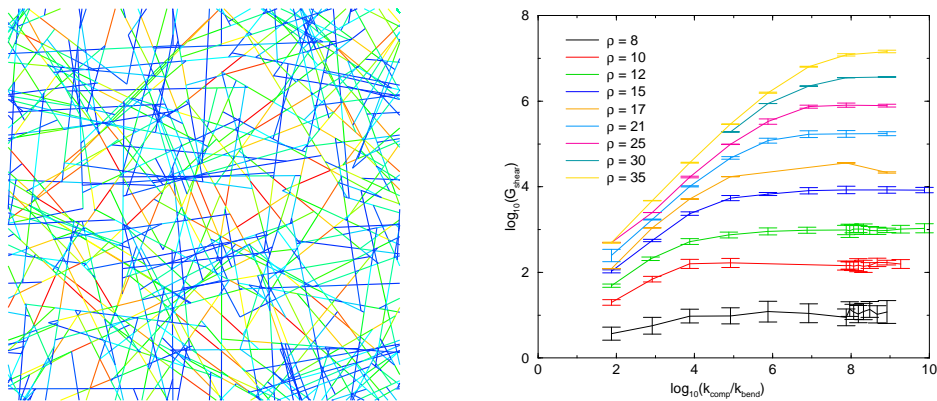


Figure 5: *Left:* Network of sticks for $\rho = 50$, $L = 2$ and $\alpha = 0.01$. The color code indicates the load distribution with energy decreasing from red to blue. *Right:* Dependence of the shear modulus on the ratio $k_{\text{comp}}/k_T/k_{\text{bend}}$ for networks with $L = 15$.

certain point the modulus ceases to depend on k_{comp} , indicating that the elasticity is dominated by bending modes. While these two-dimensional results are certainly not straightforwardly applicable to three-dimensional networks we will nevertheless try to get a feeling for the scales involved. Network densities can be compared roughly by using the average distance L_c between intersections as a measure: A cytoskeletal network might have $L_c \approx 0.1 \mu\text{m}$ with typical filament lengths of $2 \mu\text{m}$ corresponding to a two-dimensional density of $\rho \approx 20$ and an aspect ratio of $\alpha \approx 0.002$ resp. $k_{\text{comp}}/k_{\text{bend}} \approx 10^5$. Comparison with Fig. 5 shows that this would just place the network in the bending dominated regime. This might, however, be different for different scales or if more order is present in the network than assumed here. For a more detailed analysis of the random stick model see Ref. [60].

4 Summary and Future Perspectives

We have seen that the cytoskeleton is a composite biomaterial with a wide variety of interesting viscoelastic properties. In particular F-actin solutions and networks provide a model system for a polymeric liquid composed of semiflexible polymers which is accessible to a complementary set of experimental techniques ranging from direct imaging techniques over dynamic light scattering to classical rheological methods.

From these studies it has become quite obvious that semiflexible polymer networks require new theoretical models different from conventional theories for rubber elasticity. The nature of the entanglement in solutions of filaments is very different from flexible coils. In a frequency window where an elastic plateau is observed a tube picture where the modulus results from the free energy costs associated with the tube deformations seems to be sufficient to explain the observed concentration dependence of the plateau modulus and even its absolute value [53].

Outside the rubber plateau in the high-frequency as well as the low-frequency regime the situation is less clear. Micro-rheology and dynamic light scattering experiments allow us to access the short-time dynamics of the filaments within a network. Here a theoretical model which describes the combined dynamics of network and solvent in this regime is still lacking. At present there are two quite different approaches which either start from a continuum medium approximation or from a single-filament picture. Obviously both are just limiting cases and a molecular theory needs to explain how starting from the single-filament dynamics including interactions with the solvent and the neighboring filaments leads at some length and time scale to collective behavior, which might be described in terms of some continuum model.

Another very important question is concerned with the effect of chemical crosslinks on the mechanical properties of semiflexible polymer networks. This is of prime interest for both cell biology and for polymer science. In cell biology one would like to know how the material properties (e.g. elastic modulus, time scales for structural rearrangement and stress propagation) change with the network architecture and the mechanical and dynamic properties of the crosslinks. From the perspective of polymer science it connects cytoskeletal elasticity with the very active fields of transport in random media and elastic percolation. In section 3.3 we have presented a numerical study using a two-dimensional toy model. One can certainly not expect that such a simplified model leads to quantitative results, but we think that some of its main features carry over to the more complicated situation of a three-dimensional network.

Acknowledgment: This work has been supported by the Deutsche Forschungsgemeinschaft through a Heisenberg Fellowship (No. Fr 850/3) and through SFB 266 and 413.

References

- [1] O. Kratky and G. Porod, *Rec. Trav. Chim.* **68**, 1106 (1949).
- [2] K. Holmes, D. Popp, W. Gebhard, and W. Kabsch, *Nature* **347**, 44 (1990).
- [3] S. Burlacu, P. Janmey, and J. Borejdo, *Am. J. Physiol.* **C5**, 69 (1992).
- [4] A. Ott, M. Magnasco, A. Simon, and A. Libchaber, *Phys. Rev. E* **48**, R1642 (1993).
- [5] F. Gittes *et al.*, *Journal of Cell Biology* **120**, 923 (1993).
- [6] H. Isambert *et al.*, *J. Biol. Chem.* **270**, 11437 (1995).
- [7] K. Kroy and E. Frey, *Phys. Rev. E* **55**, 3092 (1997).
- [8] K. Kroy and E. Frey, in *Applications of Dynamic Light Scattering*, edited by W. Brown (Gordon and Breach, 1998).
- [9] P. A. Janmey, *Curr. Op. Cell. Biol.* **2**, 4 (1991).
- [10] K. Luby-Phelps, *Curr. Op. Cell. Biol.* **6**, 3 (1994).
- [11] E. Sackmann, *Macromol. Chem. Phys.* **195**, 7 (1994).

- [12] F. MacKintosh and P. A. Janmey, *Curr. Op. Cell. Biol.* **2**, 350 (1997).
- [13] P. A. Janmey *et al.*, *Biochemistry* **27**, 8218 (1988).
- [14] O. Müller, H. E. Gaub, M. Bärmann, and E. Sackmann, *Macromol.* **24**, 3111 (1991).
- [15] P. A. Janmey, U. Euteneuer, P. Traub, and M. Schliwa, *J. Cell. Biol.* **113**, 155 (1991).
- [16] T. D. Pollard, I. Goldberg, and W. H. Schwarz, *J. Biol. Chem.* **267**, 20339 (1992).
- [17] J. Newman *et al.*, *Biophys. J.* **64**, 1559 (1993).
- [18] P. A. Janmey *et al.*, *J. Biol. Chem.* **269**, 32503 (1994).
- [19] J. Käs *et al.*, *Biophys. J.* **70**, 609 (1996).
- [20] M. Tempel, G. Isenberg, and E. Sackmann, *Phys. Rev. E* **54**, 1802 (1996).
- [21] B. Hinner *et al.*, *cond-mat/9712037* (1997).
- [22] A. Caspi *et al.*, *Phys. Rev. Lett.* **80**, 1106 (1998).
- [23] S. M. Aharoni and S. F. Edwards, *Rigid Polymer Networks*, Vol. 118 of *Advances in Polymer Science* (Springer, Berlin, 1994).
- [24] J. L. Jones and R. C. Ball, *Macromol.* **24**, 6369 (1991).
- [25] F. MacKintosh, J. Käs, and P. Janmey, *Phys. Rev. Lett.* **75**, 4425 (1995).
- [26] H. Isambert and A. C. Maggs, *Macromol.* **29**, 1036 (1996).
- [27] K. Kroy and E. Frey, *Phys. Rev. Lett.* **77**, 306 (1996).
- [28] R. L. Satcher, Jr. and C. F. Dewey, Jr., *Biophys. J.* **71**, 109 (1996).
- [29] E. Frey, K. Kroy, J. Wilhelm, and E. Sackmann, in *Dynamical Networks in Physics and Biology*, edited by G. Forgacs and D. Beysens (Springer Verlag, Berlin, 1998).
- [30] R. Granek, *J. Phys. II France* **7**, 1761 (1997).
- [31] J. Käs, H. Strey, and E. Sackmann, *Nature* **368**, 226 (1994).
- [32] *Monte Carlo and Molecular Dynamics Simulations in Polymer Science*, edited by K. Binder (Oxford University Press, Oxford, 1995).
- [33] M. Schliwa, *The Cytoskeleton: An Introductory Survey* (Springer Verlag, Berlin, 1985).
- [34] J. Hartwig and D. Kwiatkowski, *Curr. Opinion Cell Biol.* **3**, 87 (1991).
- [35] J. Olmsted, *Annu. Rev. Cell Biol.* **2**, 421 (1986).
- [36] N. Saitô, K. Takahashi, and Y. Yunoki, *J. Phys. Soc. Jap.* **22**, 219 (1967).
- [37] H. Benoit and P. M. Doty, *J. Chem. Phys.* **87**, 958 (1953).
- [38] J. Wilhelm and E. Frey, *Phys. Rev. Lett.* **77**, 2581 (1996).
- [39] H. E. Daniels, *Proc. Roy. Soc. Edinburgh* **63A**, 290 (1952).
- [40] H. Yamakawa, *Modern Theory of Polymer Solutions* (Harper & Row, New York, 1971).
- [41] E. Frey and D. R. Nelson, *J. Phys. I France* **1**, 1715 (1991).
- [42] E. Farge and A. C. Maggs, *Macromol.* **26**, 5041 (1993).
- [43] L. Harnau, R. G. Winkler, and P. Reineker, *J. Chem. Phys.* **140**, 6355 (1996).
- [44] R. Götter *et al.*, *Macromol.* **29**, 30 (1996).
- [45] C. F. Schmidt, Ph.D. thesis, Technische Universität München, 1988.
- [46] M. Doi and S. F. Edwards, *The Theory of Polymer Dynamics* (Clarendon Press, Oxford, 1986).
- [47] G. Arcovito *et al.*, *Biophysical Chemistry* **67**, 287 (1997).
- [48] L. R. G. Treloar, *The Physics of Rubber Elasticity* (Clarendon Press, Oxford, 1975).
- [49] B. Hinner *et al.*, unpublished.
- [50] W. Helfrich and W. Harbich, *Chem. Scr.* **25**, 32 (1985).
- [51] T. Odijk, *Macromol.* **19**, 2313 (1986).
- [52] A. N. Semenov, *J. Chem. Soc. Faraday Trans.* **86**, 317 (1986).
- [53] J. Wilhelm and E. Frey, *Eur. Phys. J. B* (1998), submitted.
- [54] F. Amblard *et al.*, *Phys. Rev. Lett.* **77**, 4470 (1996).
- [55] F. Gittes *et al.*, *Phys. Rev. Lett.* **79**, 3286 (1997).
- [56] B. Schnurr, F. Gittes, F. C. MacKintosh, and C. F. Schmidt, *Macromol.* **30**, 7781 (1997).

- [57] F. Gittes and F. C. MacKintosh, unpublished.
- [58] D. Morse, unpublished.
- [59] K. Kroy and E. Frey, in preparation.
- [60] J. Wilhelm and E. Frey, in preparation.